



## ARTICLE

# Modeling and Simulation of the Deactivation by Sintering of the Cobalt Catalyst during the Fischer-Tropsch Reaction

Dounia Alihellal<sup>1</sup> Lemnouer Chibane<sup>1</sup> Mohamed El-Amine Slimani<sup>2\*</sup>

<sup>1</sup> Laboratoire de Génie des Procédés Chimiques (LGPC), Département de Génie des Procédés, Faculté de Technologie, Université Ferhat Abbas Sétif 1, UN1901 Sétif, Algeria

<sup>2</sup> Department of Energetic and Fluid Mechanics, Faculty of Physics, University of Science and Technology Houari Boumediene (USTHB), 16111 Algiers, Algeria

### ARTICLE INFO

#### Article history

Received: 5 November 2018

Accepted: 25 February 2019

Published Online: 12 March 2019

#### Keywords:

Clean fuels

Fischer-Tropsch process

Cobalt catalysts

Deactivation by sintering

The Fischer

### ABSTRACT

In the present work, the deactivation by sintering of cobalt based catalyst during Fischer-Tropsch synthesis at low temperature was studied by numerical simulation. For this purpose, a mathematical model was developed. The obtained simulation results allowed us to highlight and improve the understanding of the deactivation phenomena of cobalt based Fischer-Tropsch catalysts by sintering. The main results also show that the sintering phenomenon is strongly dependent on the operating conditions, in particular, the temperature, the pressure, and the H<sub>2</sub>/CO molar ratio, as well as the reaction by-products such as water. The results obtained can, therefore, be used to understand more the sintering mechanism which may be linked to the change in the concentration of the active sites and the reaction rates.

## 1. Introduction

The Fischer-Tropsch process is a catalytic process that allows the production of liquid hydrocarbons of high quality starting from a mixture of synthesis gas coming primarily from natural gas, coal or biomass<sup>[1]</sup>. In this chemical process, the most current catalysts are iron, cobalt<sup>[2]</sup>, ruthenium, as well as nickel<sup>[3]</sup>. The deactivation of cobalt catalyst during the Fischer-Tropsch synthesis at low temperature can be related to various phenomena, for example, with sintering, the oxidation of active metal, the interaction between the metal and the support and with the carbon deposit<sup>[4-6]</sup>. Most of these cases have been

addressed in previous studies. In summary, James Pater-son et al<sup>[7]</sup> studied the effect of water on the reduction of cobalt oxides. Andre P. Steynberg et al<sup>[8]</sup> have described Fischer-Tropsch catalyst deactivation in commercial microchannel reactor operation. Similarly, Ali Nakhaei Pour et al.<sup>[9]</sup> studied the deactivation of Co/CNTs catalyst in Fischer-Tropsch synthesis. Similarly, D.J. Moodley et al<sup>[10]</sup> investigated about the impact of cobalt aluminate formation on the deactivation of cobalt-based Fischer-Tropsch synthesis catalysts. Also, Erling Rytter and Anders Holmen<sup>[11]</sup> reviewed, the deactivation and regeneration of commercial type Fischer-Tropsch Co-catalysts. Alexandre Carvalho et al<sup>[12]</sup> studied the deactivation phenomena

\*Corresponding Author:

Mohamed El-Amine Slimani,

Department of Energetic and Fluid Mechanics, Faculty of Physics, University of Science and Technology Houari Boumediene (USTHB), 16111 Algiers, Algeria

Email: [muslimani@usthb.dz](mailto:muslimani@usthb.dz)

in cobalt catalyst for Fischer-Tropsch synthesis using SSITKA. And Christine Lancelot et al [13] gives a direct evidence of surface oxidation of cobalt nanoparticles in alumina-supported catalysts for Fischer-Tropsch synthesis.

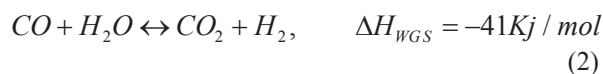
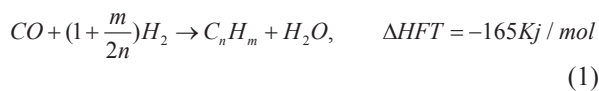
Sintering could be the principal cause of the initial deactivation, which continues in the long run with the phenomenon of coking. This phenomenon has been addressed by many researchers. Kamyar Keyvanloo et al [14] studied the kinetics of deactivation by carbon of a cobalt Fischer-Tropsch catalyst under the effects of CO and H<sub>2</sub> partial pressures. Majid Sadeqzadeh et al [15,16] addressed this phenomenon in detail in their two papers entitled mechanistic modeling of cobalt based catalyst sintering in a fixed bed reactor under different conditions of Fischer-Tropsch synthesis, and deactivation of a Co/Al<sub>2</sub>O<sub>3</sub> Fischer-Tropsch catalyst by water-induced sintering in slurry reactor: Modeling and experimental investigations.

In this work, we studied by numerical simulation the phenomenon of cobalt catalyst deactivation by sintering during the synthesis of Fischer-Tropsch in a tubular fixed bed reactor. The effect of some parameters operational on the performances of the process was examined.

## 2. Mathematical Model

### 2.1 Fischer-Tropsch Reaction

The synthesis of Fischer-Tropsch it is a chemical reaction allows synthesizing hydrocarbons from a mixture of carbon monoxide and hydrogen according to the following reactions [16]:



Where the first reaction is the reaction of Fischer-Tropsch and the second reaction is the reaction of water-Gas-Shift.

### 2.2 Fischer-Tropsch Reaction Kinetics

Among the kinetic models describing the rate of the Fischer-Tropsch synthesis on a cobalt-based catalyst, we have the model of the Langmuir-Hinshelwood type illustrated by Yates and Satterfield [17]:

$$R_{FT} = -R_{CO} = \frac{aP_{CO}P_{H_2}}{(1 + bP_{CO})^2} \quad (3)$$

$a$  and  $b$  are temperature dependent constants representing a kinetic parameter and an adsorption coefficient.

For the reaction of water-gas-shift the kinetic model used is represented by the equation following [18]

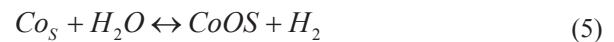
$$R_{WGS} = K_{WGS} \frac{(P_{CO}P_{H_2O} - \frac{P_{CO_2}P_{H_2}}{K_1})}{(P_{CO} + K_2P_{H_2O})} \quad (4)$$

**Table 1.** Kinetic parameters of cobalt catalyst

| Parameter                                      | Value  |
|--|--------|
| K WGS (mol.kg <sup>-1</sup> .s <sup>-1</sup> ) | 0.0292 |
| K1   | 85.81  |
| K2   | 3.07   |

### 2.3 Deactivation of Cobalt Catalyst by Sintering

The suggest that the first stage of sintering of cobalt in the presence of water could cause reversible surface oxidation of the cobalt nanoparticles:



The following equation gives the diffusion coefficient of the Co particles in the alumina support:

$$D_i = 4.818D_s \left(\frac{2r}{d_i}\right)^4 \quad (6)$$

Equation (7) makes it possible to calculate the surface coverage rate  $\theta_{CoO}$  by CoO:

$$\theta_{CoO} = K_{CoO} \frac{P_{H_2O}}{P_{H_2}} \quad (7)$$

$$K_{CoO} = \frac{\theta_{CoO}}{1 - \theta_{CoO}} \left(\frac{P_{H_2}}{P_{H_2O}}\right)^{(\theta_{CoO} \ll 1)} \theta_{CoO} \frac{P_{H_2}}{P_{H_2O}} \quad (8)$$

The evolution of the average diameter of the particles of Co according to time is a function of the ratio H<sub>2</sub>O/H<sub>2</sub> of partial pressure during sintering [19]:

$$\bar{d}_s = \left[ \frac{1}{1.28 * 10^{-4} - 5k_s \frac{P_{H_2O}}{P_{H_2}} t} \right]^{1/5} \quad (9)$$

The concentrations are used because this reaction can be limited by the external mass transfer in the industrial reactors [19].

**Table 2.** Operating conditions of the simulation

| Parameter   | Value                 |
|---|-----------------------|
| $\bar{k}_a$ (m <sup>7</sup> /kg <sub>cat</sub> .mol.h)) | 4.62*10 <sup>-8</sup> |
| $K_b$ (m <sup>3</sup> /mol)                             | 0.342                 |
| Pressure (bar)  | 20                    |
| Temperature (K)   | 503                   |
| H <sub>2</sub> /CO                                      | 2-3.2                 |

$$R_{FT} = \frac{1}{\bar{d}_s} \frac{kaC_{CO}C_{H_2}}{(1+k_bC_{CO})^2} \quad (10)$$

$$k_a = \left( \frac{3}{2r^2 N_{AV} \rho_{Co}} \right) \bar{k}_a \quad (11)$$

**Table3.** Principal characteristics of the catalyst

| Parameter      | Value      |
|----------------|------------|
|                | 8900       |
|                | 6          |
| ks(nm7/s)      | 29.68      |
| ds(m2/s)       | 3.3*10-18  |
| r(nm)          | 0.125      |
|                | 0.9        |
| Nav(atoms/mol) | 6.023*1023 |
| Ks(nm7/s)      | 29.68      |

## 2.4 Model of Reactor Studied

The geometry of the reactor used consists of a tubular reactor with a fixed bed (figure 1) through which a gas mixture (CO and H<sub>2</sub>) passes in flow piston. The industrial catalyst containing cobalt Co/Al<sub>2</sub>O<sub>3</sub> (15% in weight of Co) which is tested under commercial conditions of FT (220°C, 20 bar and H<sub>2</sub>/CO=2) is distributed in the catalytic zone over a length of 9mm of the catalytic bed. The diagram of the reactor and different parameters of the reactor as well as the properties of catalysts and gases of synthesis are given respectively by Figure 1 and Table 4.

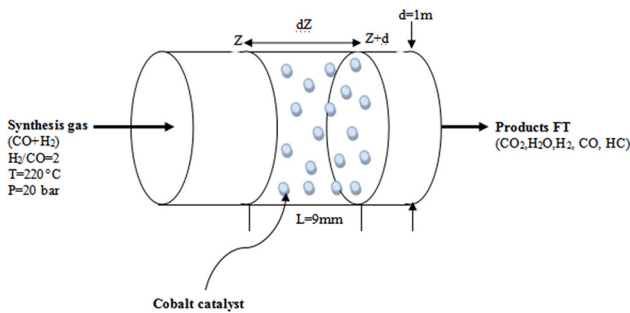


**Figure 1.** Representative configuration of the studied reactor

**Table 4.** Reactor parameters, properties of catalyst and gas

| <u>Reactor parameters</u>    |          |
|------------------------------|----------|
| Catalytic bed length(mm)     | 9        |
| Reactor diameter(mm)         | 1        |
| Initial total pressure (bar) | 20       |
| Initial temperature(°c)      | 220      |
| <u>Catalyst properties</u>   |          |
| Density(kg/m3)               | 2030     |
| Particules diameter (m)      | 5x10-4   |
| <u>Gas properties</u>        |          |
| Viscosity (Pa.s)             | 1.8x10-5 |
| Gas density (kg/m3)          | 13.2     |

### Material balance

$$\frac{dF_i}{dz} = \rho A \sum v_{ij} \cdot R_i, \quad (12)$$

By using the following definition of conversion X<sub>FTS</sub> and X<sub>WGS</sub> we can write for carbon monoxide and hydrogen:

$$X_{CO} = \frac{F_{CO}^0 - F_{CO}}{F_{CO}^0} \quad (13)$$

$$X_{H_2} = \frac{F_{H_2}^0 - F_{H_2}}{F_{H_2}^0} \quad (14)$$

After mathematical arrangements and by the introduction of the dimensionless length (l) we obtain:

$$\frac{dX_{FTS}}{dl} = \frac{\rho AL}{F_{CO}^0} R_{FTS} \quad (15)$$

$$\frac{dX_{WGS}}{dl} = \frac{\rho AL}{F_{CO}^0} R_{WGS} \quad (16)$$

### Partial pressures

$$P_i = \frac{F_i}{F_T} \cdot P_T, \quad (17)$$

The total molar flow in the reactor can be evaluated by the following expression:

$$F_T = F_T^0 - F_{CO}^0 (X_{FTS} + Y_{H_2O}) \quad (18)$$

The total molar flow rate at the reactor inlet is calculated using the ideal gas law:

$$P_T Q = F_T^0 RT, \quad (19)$$

The volumetric flow is given by:

$$Q = vA \tag{20}$$

Therefore, the total initial molar flux can be expressed as follows:

$$F_T^0 = \frac{P_T v A}{RT} \tag{21}$$

On the other hand, the total molar flow rate at the inlet of the reactor is given by:

$$F_T^0 = F_{CO}^0 + F_{H_2}^0 \tag{22}$$

The molar feed ratio between hydrogen and carbon monoxide is denoted by (M). This report is defined as follows:

$$M = \frac{F_{H_2}^0}{F_{CO}^0} \tag{23}$$

Thus, the carbon monoxide input molar flux can be evaluated according to the following equation:

$$F_{CO}^0 = \frac{P_T^0}{1 + M} \tag{24}$$

**Hypotheses**

- a. Typical low temperature FT conditions (20 bar, 220 °C) are applied.
- b. The perfect gas law is used as the equation of state.
- c. Mass transfer limits are considered negligible under these conditions.
- d. The parameters can then be calculated according to the axial position of the reactor.
- e. The model is considered under isothermal conditions: The catalyst particles and the reagents are assumed at the same temperature: The thermal balance expression is not necessary in this case.
- f. The reactor operates in fixed bed mode and steady state is established.

**3. Results and Discussion**

**3.1 Effect of the Total Pressure Initial**

**3.1.1 On the FT and WGS Reactions Rates**

The results obtained are presented in a comparative way between the two cases studied: in the absence and the presence of sintering during the unfolding of the chemical reaction. For the reaction of FT (Figure 2 (a)), it notes that an increase in the rate with the increase in the pressure in both cases in the absence and in the presence of sintering.

Nevertheless, in the presence of sintering the rate of FT decreases in a remarkable way where one records with 20 bars a value of  $4.3 \cdot 10^{-3}$  mol/kg-1/s-1 in the absence of sintering, whereas in the presence of sintering, speed decreases until  $7.9 \cdot 10^{-4}$  mol/kg-1/s-1.

The effect of the pressure on the reaction rate of WGS also is studied and presented on (Figure 2 (b)), which one notes an increase in the rate with the increase in pressure in the presence of sintering and decreases in the absence of sintering.

The FT reaction rate is dependent on the pressure of CO and H<sub>2</sub>. It has been noticed that the increase of the pressure causes an increase of the rate. But in the presence of sintering the reaction rate is decreased because of the increase of the multiplicative factor relating to sintering. On the other hand the WGS reaction rate is independent of the sintering and depends only on the pressure which causes an increase of the rate with the pressure.

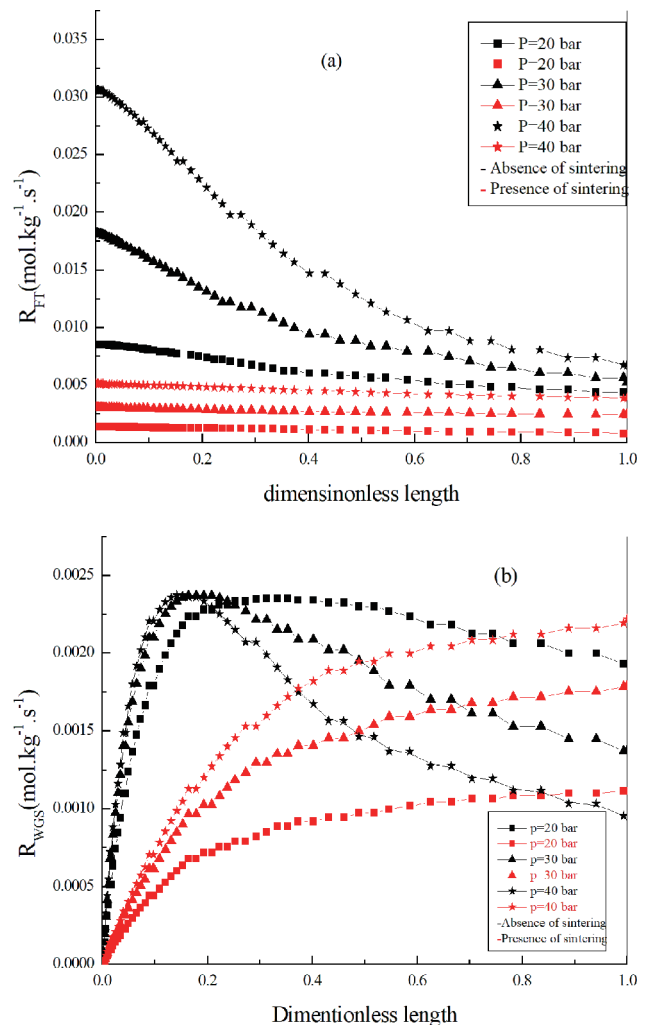


**Figure 2.** Effect of the total initial pressure on the reactions rates FT (a) and WGS (b) (Conditions: T = 220 °C, H<sub>2</sub>/CO=2)

### 3.1.2 On the Conversion of FT and WGS Reactions

According to the Figure 3 (a) it notes that the increase in the pressure leads to an increase in the conversion of CO in the reaction of FT for the two cases in the absence and the presence of sintering. But with the sintering of the catalyst the increase of the conversion is less important compared to that without sintering.

For the conversion of CO in the reaction of WGS one observes an effect of pressure opposite compared to that in the reaction of FT. Where the results of Figure 3 (b) show an increase in conversion with the pressure decrease, which means that the reaction of WGS is favorable there in this case by the low pressures. So in the presence of sintering the increase is less important

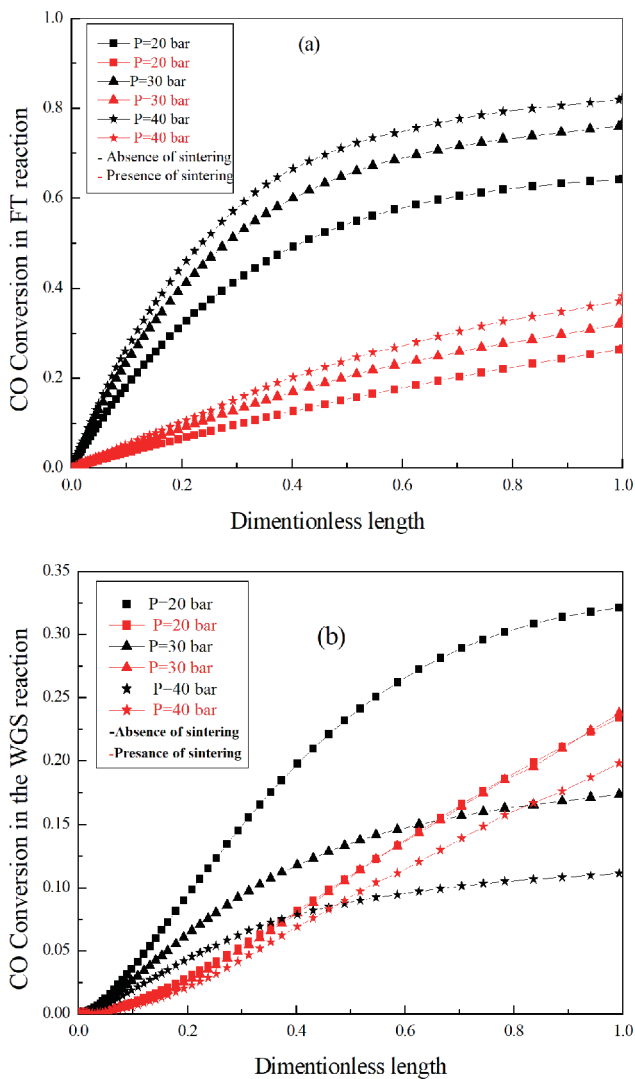


**Figure 3.** Effect of the total initial pressure on the conversion of CO in the FT reaction (a) and the WGS reaction (b) (Conditions:  $T=220\text{ }^{\circ}\text{C}$ ,  $\text{H}_2/\text{CO}=2$ )

### 3.2 Effect of the Molar Ratio $\text{H}_2/\text{CO}$

#### 3.2.1 On the Reactions of FT and WGS Rates

According to the results obtained, it shows that the increase in  $\text{H}_2/\text{CO}$  molar ratio (Figure 4 (a)) leads to a remarkable reduction in the reaction rate in the absence of sintering and a weak lowering in the presence of sintering. This is due to the decrease in the pressure of the two reactants CO and  $\text{H}_2$  which cause the decrease of the reaction rate.

According to Figure 4 (b) it notes that the WGS reaction rate increases with the increase in  $\text{H}_2/\text{CO}$  molar ratio in the presence or the absence of sintering. Nevertheless in the presence of sintering the increase is less significant compared to that obtained in the absence of sintering.

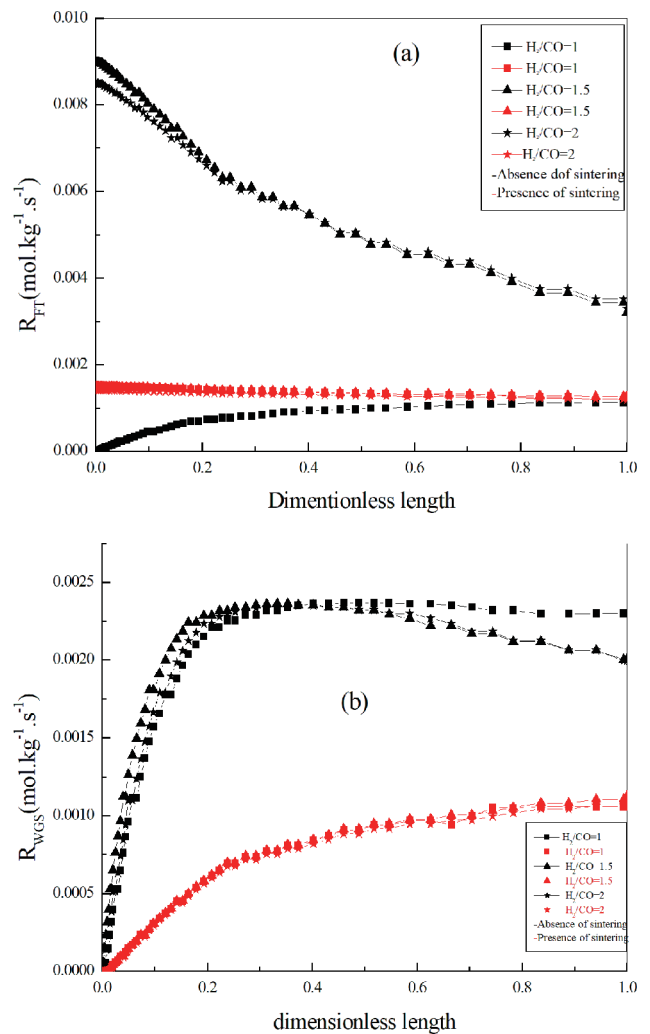


**Figure 4.** Effect of the  $\text{H}_2/\text{CO}$  molar ratio on the reactions rates  $R_{FT}$  (a); and on the  $R_{WGS}$  (b) according to the length of reactor (Conditions:  $T=220\text{ }^{\circ}\text{C}$ ,  $P=20\text{ bar}$ )

#### 3.2.2 On the Conversion of Reactions FT and WGS

The principal results obtained (Figure 5(a) and (b)) show

that the conversion of CO in the reaction of FT and WGS increases with the increase in molar ratio  $H_2/CO$  in the absence and the presence of sintering. However, the best performances are increasingly more significant in the lack of sintering and with a value of  $H_2/CO$  ratio equal to 2 (typical case of the GTL) in the two reactions of FT and WGS. Therefore, it can conclude that the sintering is actively contributed to the reduction in total conversion by a rate of 56%.

The two expressions of the conversion rates of Ft and WGS are dependent on the molar flow of the two reactants CO and  $H_2$ , so each increase in ratio M involved an increase in the conversion.

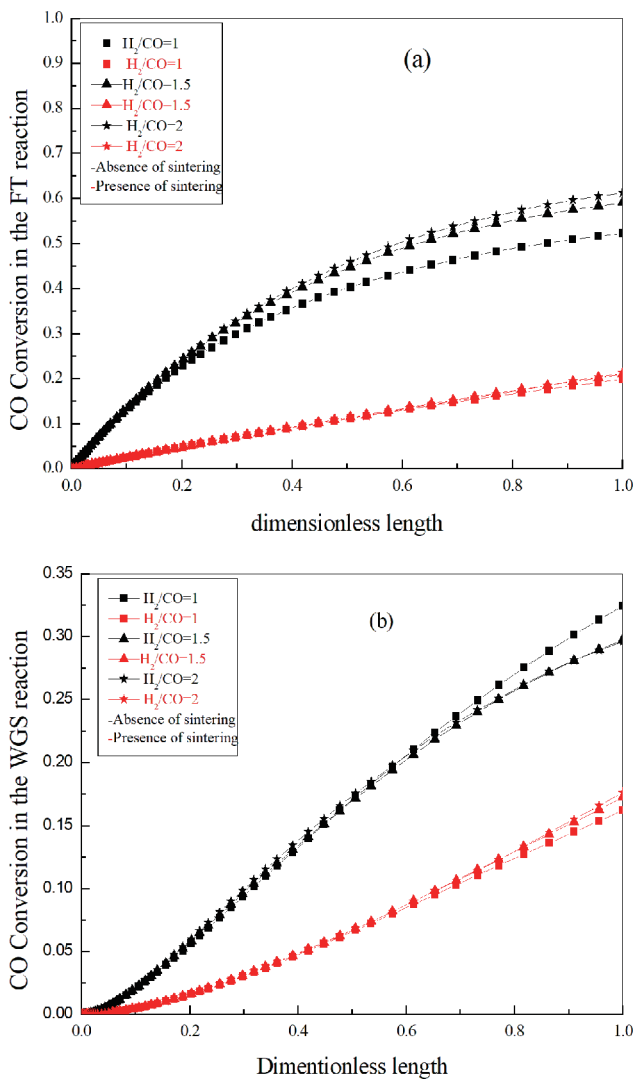


**Figure 5.** Effect of the  $H_2/CO$  molar ratio on the reactions conversions FT (a) and on the WGS (b) according to the length of reactor (Conditions: T 220°C, P = 20 bar)

### 3.3 Effect of the Reaction Temperature

#### 3.3.1 On the FT and WGS Reactions Rates

The study is conducted at low temperatures: 220, 230 and 240 °C (LFT and LWGS). The results obtained are represented in Figure 6. From these results, it notes that the increase in the temperature leads to a reduction the FT reaction rate (Figure 6(a)) in both cases in the absence and in the presence of sintering, which shows that the reaction is unfavorable by the high temperatures. For example at 240 °C, the reaction rate decreases from 0.008 mol/kg-1/s-1 to 0.0031 mol/kg-1/s-1 in the absence of sintering and 0.0014 mol.kg-1.s-1 to 0.0011mol/kg-1/s-1 in the presence of sintering.

Nevertheless the WGS reaction rate increases as the temperature increases (Figure 6 (b)) in the presence and absence of sintering, which shows that the reaction of WGS is favorable for the high temperatures.

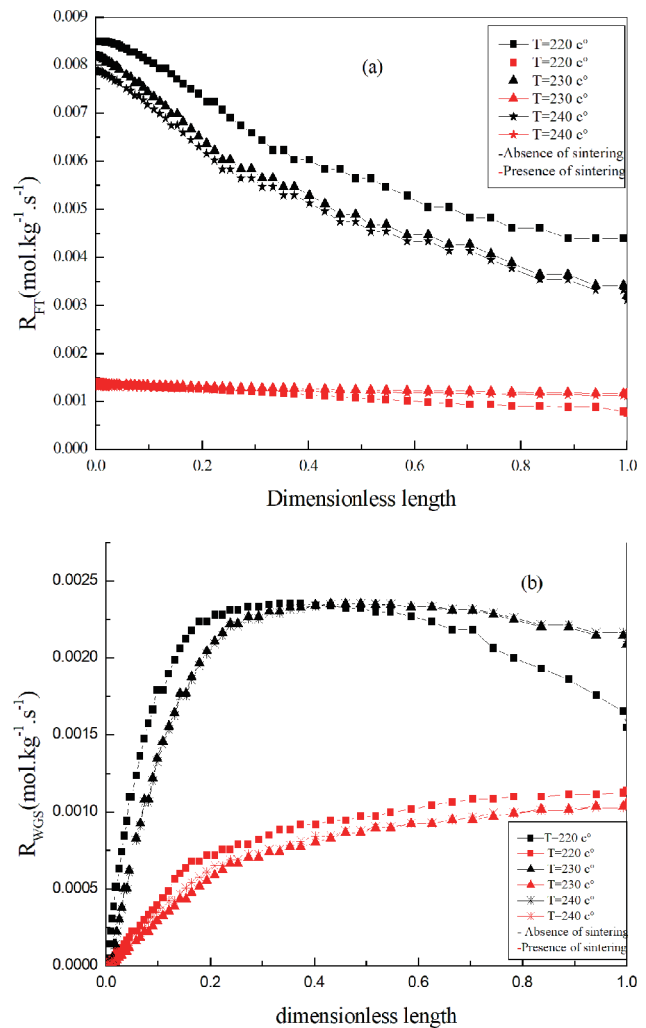


**Figure 6.** Effect of the temperature on the FT reaction rate (a) and on the WGS reaction rate (b) (Conditions:  $H_2/CO=2$ , P = 20 bar)

#### 3.3.2 On the FT and WGS Conversion Reactions

Figure 7 presents a comparison between the conversions

of CO obtained in the two reactions FT (Figure 7 (A)) and WGS (Figure 7 (b)) in the event of the absence of sintering and after its appearance. According to the results obtained for the reaction of FT, it notes a weak improvement of the conversion with the increase in temperature in the case of absence and the presence of sintering. Although after sintering, we observe conversions less important than those obtained before sintering. For the three temperatures examined, the increase in the conversion is not very important; rates are almost close to 63%-64% in the absence of sintering and close to 25% -26% in the presence of sintering of the catalyst.

For the reaction of WGS, the effect of the temperature on the CO conversion is identical to this in the reaction of FT. where there are very similar conversions in the two cases studied. In the presence of sintering, a conversion of 23% is completed for the three temperatures. Moreover, the results obtained in the absence of sintering show the possibility of having the following conversions: 32%, 33% and 34%, respectively for the three temperatures examined.

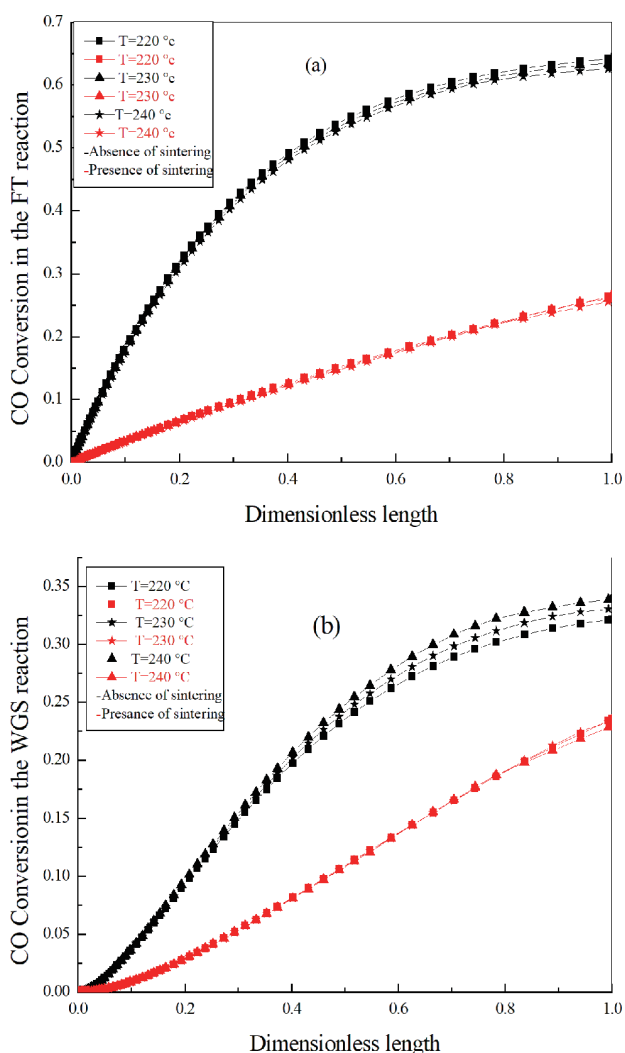


**Figure 7.** Effect of the temperature on the CO conversion on FT reaction (a) and on the WGS reaction (b) (Conditions:  $H_2/CO=2$ ,  $P = 20$  bar)

#### 4. Conclusion

The main results obtained through this study are very interesting. The contribution suggests that the partial pressure ratio water-hydrogen may drive sintering and therefore higher sintering is expected under all high conditions of  $H_2/CO$  ratio and temperature. In general, the operation of the process under the effect of specific operating parameters can ensure increasing conversions of CO. Sintering is driven by thermodynamic reasons because the larger crystallites have lower surface energy and therefore greater thermodynamic stability. The formation of the CoO layer contributes to reducing both the surface energy and increases the mobility of the small crystallites Co and thus increases the sintering rate. The crystalline growth of cobalt is also accelerated by the water produced during FT synthesis. Therefore, to fight against this phenomenon, the removal of this water by the use of a membrane reactor makes it possible to minimize the deactivation by sintering.

#### Nomenclature

|          |   |
|----------|---|
| a        | cobalt crystallite surface ( $m^2$ )  |
| A        | surface area per mole of surface atoms ( $m^2 / \text{mole}$ )                  |
|          | number-average Co crystallite diameter (nm)                                     |
| ds       | average diameter of the surface of the cobalt crystalline (nm)                  |
| Fi       | Molar flow rate of component i (mol/h)  |
| $H_2/CO$ | The molar ratio of hydrogen to carbon monoxide in synthesis gas                 |
| Ka, kb,  | The kinetic parameters (unit depends on the kinetic law in which they are used) |
| n        | number of carbon atoms in the hydrocarbon produced by FT $C_nH_{2n+2}$          |
| NAV      | The number of Avogadro ( $6,022 \times 10^{+23}$ atoms / mole)                  |
| P        | Pressure (bars)   |
| r        | Co-Co interatomic distance, 0,125 nm  |

#### Rate of reaction number i

|     |                  |
|-----|------------------|
| T   | Temperature (K)  |
| XCO | Conversion of CO |
| XH2 | Conversion of H2 |

**Acronyms**

|     |                           |
|-----|---------------------------|
| FT  | Fischer-Tropsch           |
| FTS | Fischer-Tropsch Synthesis |
| WGS | Water-Gas-Shift           |

**Greeksymbols**

|             |   |
|-------------|---|
| $\rho_c$    | The density of catalyst (kg/m <sup>3</sup> )        |
| $\rho_{Co}$ | The density of cobalt catalyst (kg/m <sup>3</sup> ) |

 **$\theta_{CoO}$** 

|                |   |
|----------------|---|
| $\theta_{CoO}$ | surface coverage CoO on cobalt crystallites (dimensionless) |
| $\nu$          | stoichiometric coefficient                                  |

**Subscripts**

|   |                    |
|---|--------------------|
| 0 | Initial conditions |
| i | chemical species   |

**References**

- [ 1 ] W. Chen, T. Lin, Y.dai, Y.An, F.Yu, L.Zhong, S. Li, Y.Sun, "Recent advances in the investigation of nanoeffects of Fischer-Tropsch catalysts," *Catal. Today*.311 (2018): 8-22
- [ 2 ] L.Guo ,J.Sun ,J.Wei , Z. Wen, H.Xu ,Q.Ge, " Fischer-Tropsch synthesis over iron catalysts with corn-cob-derived promoters," *J. Energy Chem.* 26 (4) (2017): 632-638
- [ 3 ] S.Golestan, A.A.Mirzaei, H.Atashi, "Kinetic and mechanistic studies of Fischer-Tropsch synthesis over thenano-structured iron-cobalt-manganese catalyst prepared by hydrothermal procedure," *Fuel*, 200 (2017): 407-418
- [ 4 ] W. Ma, G. Jacobs, V. R. R.Pendyala, D. E. Sparks, W. D. Shafer, G. A. Thomas, A. MacLennan, Y. Hu, B. H. Davis, "Fischer-Tropsch synthesis. Effect of KCl contaminant on the performance of iron and cobalt catalysts," *Catal.Today*.299 (2018): 28-361
- [ 5 ] N. E. Tsakoumis, M.Ronning, O. Borg, E.Rytter, A. Holmen, "Deactivation of cobalt based Fischer-Tropsch catalysts: A review," *Catal.Today*.154 (2010): 162-182
- [ 6 ] N. E. Tsakoumis, A.Voronov, M.Ronning, W. van Beek, O.Borg,E.Rytter, A. Holmen, "Fischer-Tropsch synthesis: An XAS/XRPD combined in situ study from catalyst activation to deactivation," *J. Catal.*291(2012): 138-148
- [ 7 ] J. Paterson , M. Peacock , E. Ferguson , M. Ojeda , J. Clarkson, "In Situ X-ray Diffraction of Fischer-Tropsch Catalysts-Effect of Water on the Reduction of Cobalt Oxides," *Appl. Catal. A- Gen.* 546 (2017): 103-110
- [ 8 ] P. A. Steynberg, S. R. Deshmukh, H. J. Robota, "Fischer-Tropsch catalyst deactivation in commercial microchannel reactor Operation, " *Catal. Today*, 299 (2018):10-13
- [ 9 ] A. Nakhaei Pour, S. Ali Taheri, S. Anahid, B. Hataami, A. Tavasoli, "Deactivation studies of Co/CNTs catalyst in Fischer-Tropsch synthesis, " *J Na. Gas Sci Eng.* 18 (2014): 104-111
- [10] D.J. Moodley, A.M. Saib, J. van de Loosdrecht, C.A. Welker-Nieuwoudt, B.H. Sigwebela, J.W. Niemantsverdriet, "The impact of cobalt aluminate formation on the deactivation of cobalt-based Fischer-Tropsch synthesis catalysts," *Catal. Today*. 171 (2011): 192-200
- [11] E. Rytter, A. Holmen, "Deactivation and Regeneration of Commercial Type Fischer-Tropsch Co-Catalysts-A Mini-Review, " *Catal.* 5 (2015): 478-499
- [12] A. Carvalho, V. V. Ordonsky, Y. Luo, M. Marinova, A. R. Muniz, N. R. Marcilio, A. Y. Khodakov, "Elucidation of deactivation phenomena in cobalt catalyst for Fischer-Tropsch synthesis using SSITKA, " *J. Catal.* 344 (2016): 669-679
- [13] C. Lancelot, V. V. Ordonsky, O. S. M. Sadeqzadeh, H. Karaca, M. Lacroix, D. Curulla-Ferré, F. Luck, P. Fongarland, A. Griboval-Constant, A. Y. Khodakov, "Direct Evidence of Surface Oxidation of Cobalt Nanoparticles in Alumina-Supported Catalysts for Fischer-Tropsch Synthesis, " *ACS Catal.* 4 (2014):4510-4515
- [14] K. Keyvanloo, M.C.J. Fisher, W.C. Hecker, R. J. Lancee, G. Jacobs, C. H. Bartholomew, "Kinetics of deactivation by carbon of a cobalt Fischer-Tropsch catalyst: Effects of CO and H<sub>2</sub> partial pressures, " *J. Catal.* 327 (2015): 33-47
- [15] M. Sadeqzadeh, J. Hong, P. Fongarl, D. Curulla-Ferré, F. Luck, J. Bousquet, D. Schweich, A.Y. Khodakov, "Mechanistic Modeling of Cobalt Based Catalyst Sintering in a Fixed Bed Reactor under Different Conditions of Fischer-Tropsch Synthesis," *Ind. Eng. Chem. Res.* 51(2012): 11955-11964
- [16] A. K. Dalai, T. K. Das, K. V. Chaudhari, G. Jacobs, B. H. Davis, "Fischer-Tropsch synthesis: Water effects on Co supported on narrow and wide-pore silica, " *Appl. Catal. A- Gen.*289 (2) (2005): 135-14210
- [17] I. C. Yates, C. N. Satterfield, "Intrinsic Kinetics of the Fischer-Tropsch Synthesis on a Cobalt Catalyst," *Enrg.Fuel.* 5 (1991): 168-173
- [18] L. C. A. Mazzone, F. A. N. Fernandes, "Modeling of Fischer-Tropsch synthesis in a tubular reactor," *Lat-*

in. Am. Appl. Res. 36 (2006): 141-148

- [19] M. Sadeqzadeh, S. Chambrey, S. Piche, P. Fongarland, F. Luck, D. Curulla-Ferre, D. Schweich, J. Bousquet, A.Y. Khodakov, "Deactivation of a Co/

Al<sub>2</sub>O<sub>3</sub> Fischer-Tropsch catalyst by water-induced sintering in slurry reactor: Modeling and experimental investigations," *Catal. Today*, 215 (2013): 52-59